Received: 21 July 2020 | Revised: 19 January 2021 | Accepted: 7 March 2021

DOI: 10.1002/we.2638

RESEARCH ARTICLE

WILEY

Development and testing of a three-dimensional ballistics model for bat strikes on wind turbines

Shivendra Prakash[1,2] | Corey D. Markfort[1,2]

[1]IIHR-Hydroscience and Engineering, The University of Iowa, Iowa City, Iowa, USA

[2]Civil and Environmental Engineering, The University of Iowa, Iowa City, Iowa, USA

Correspondence
Corey D. Markfort, IIHR-Hydroscience and Engineering, The University of Iowa, Iowa City, IA 52242, USA.
Email: corey-markfort@uiowa.edu

Funding information
MidAmerican Energy Company (MEC)

Abstract

Bats colliding with spinning wind turbine blades result in bat mortality. Carcass surveys at individual wind turbines vary from daily to once a week and from large cleared plots to only the road and pad area. A physics-based model is proposed to guide carcass surveys, for designing curtailment studies to detect treatment fatalities and for improving fatality estimates by accounting for unsearched areas. The model considers the effects of carcass size, weight, and drag, and it accounts for the turbine rotor size and rotation rate to simulate the trajectory of a carcass after it is struck by a wind turbine blade. A carcass parameter is defined as the ratio of drag force to body weight, which accounts for the relative effect of bat biophysical and aerodynamic characteristics. By applying restrictions on carcass survey and turbine yaw data, a limited sample of bat fatalities was obtained, and the analysis revealed that bats fall downwind of wind turbines, indicating wind drift significantly influences carcass fall trajectories. The new ballistics model includes the effect of wind drift on fall trajectory of a carcass. The model was used to investigate the sensitivity of carcass fall trajectories to variability of the input parameters. The tests showed that larger values of the carcass parameter, that is, when drag dominates, such as for small carcasses, resulted in larger downwind drift, whereas large carcasses with smaller carcass parameter values resulted in larger distances within the rotor plane. The relationship of wind speed and RPM was found to influence the carcass downwind distance more compared to the within rotor plane distance. Using carcass survey data, turbine operation data, and wind speed records, for seven bats surveyed the day after colliding with a wind turbine, modelled back-trajectories were used to identify the likely strike location on the rotor. The model can be improved by validating the modelled trajectories with the recorded bat-blade strikes in thermal videos. It should be noted that the findings of the present study are based on the bat fatalities that met strict criteria leading to small sample size and hence requires further evaluation for testing the robustness of the model.

KEYWORDS
ballistics model, bat strike, environmental monitoring, SCADA, wind drift, wind turbine

1 | INTRODUCTION

Global electric generation from wind energy has the potential to mitigate carbon dioxide emissions.[1,2] However, with the expansion of wind power plants, bat fatalities due to collisions with turbine blades are a growing concern.[3–6] In fact, in North America, bat carcasses have been found at wind turbine facilities wherever data are available.[7,8] Several studies[9–11] have estimated large number of bat fatalities annually due to bats colliding with rotating turbine blades in North America. Using population projection models, Frick et al[12] demonstrated the increased risk of extinction of the hoary bat population in the next 50 years. The installed wind power capacity in the United States was 51,630 MW in 2012 and increased to 100,125 MW by September 2019.[13] Smallwood and Bell[14] argued that bat fatalities in the United States likely increased as wind energy capacities doubled from year 2012 to 2020. A significant number of bat fatalities at wind turbines in North America include the eastern red bat (*Lasiurus borealis*), the hoary bat (*Lasiurus cinereus*) and the silver-haired bat (*Lasionycteris noctivagans*).[15] However, the impact of wind plant projects on bat population is not limited to North America. Other regions have also recorded bat fatalities due to wind energy development, including South America,[16] Eurasia,[17] Africa[18] and Australia and New Zealand.[19]

The risk of fatality when a bat enters the rotor-swept region and the fate of carcasses after collision with wind turbine blades is necessary to evaluate the environmental impacts of wind energy projects. A robust methodology for simulating the fate of various bat species after impact with utility-scale wind turbines under varying operational conditions is needed to guide carcass surveys, estimate the total amount of fatalities, and improving fatality estimates by accounting for limited or unsearched areas. Previous studies have investigated the fall trajectory of objects including bat and bird carcasses, ice fragments, and parts of broken blades, thrown from turbine blades using ballistics theory with varying levels of detail and complexity.

Hull and Muir[20] (hereafter referred to as HM10) proposed a ballistics model to estimate the fall zone distribution of different sized bird and bat carcasses after colliding with different sized wind turbines. Their two-dimensional (2-D) ballistics model describes the carcass fall trajectory in the plane of the turbine rotor. The HM10[20] model assumes that the carcasses are stationary in the rotor plane before being hit by the blade and calm conditions, resulting in no wind drift effects on the carcass' as they fall toward the ground. HM10[20] assumed the drag coefficient (C_d) for bat carcasses as one with a range between 0.875 and 1.125 to compute the aerodynamic drag force, and a coefficient of restitution (e) of zero. The output from the HM10[20] is a one-dimensional (1-D) fall distributions of carcasses from the tower to the edge of the blades, along the rotor plane. They found the maximum distance travelled by a bat carcass for the large wind turbine of 55-m radius and 94-m hub height was 75 m from the turbine base.

Biswas et al[21] proposed a three-dimensional (3-D) ice throw model to compute the landing positions of ice fragments thrown from wind turbines and conducted a sensitivity analysis of the trajectory with respect to the input parameters. They assumed a drag coefficient of unity and coefficient of restitution of zero. For compact ice fragments, the combination parameter defined as ice fragment parameter, which is the product of fragment drag coefficient and projected area divided by the mass of the fragment, along with wind speed, fragment ejection position along the blade and blade rotation rate, were found to affect the ice fragment fall position. They found that compact ice fragments fall further away from the turbine base along the rotor plane and further in the downwind distance for high drag coefficient. The effect of lift force was considered insignificant for compact ice fragments. It was found that for a turbine with 45-m long blades and hub height of 100 m, the ice fragments could travel up to 350 m from turbine base.

Sarlak and Sørensen[22] investigated fall aerodynamics of thrown blade fragments from a 2.3-MW horizontal axis wind turbine of radius 45 m and hub height of 100 m, resulting from blade failure. They analysed the effects of detachment size and release angle, incoming wind velocity, and tip speed on the travel distance. They found tip speed at the moment of release, to be the most important factor governing the throw distance. The normal operating condition resulting in the tip speed of 70 m/s caused the thrown fragments of different sizes to travel a distance between 100 and 500 m.

Behaviour of bats near wind turbines has also been studied to better understand what factors might contribute to bat mortalities in wind farms. Cryan et al[23] investigated the behaviour of bats in the rotor-swept zones at three experimentally manipulated wind turbines in Indiana, USA. Using infrared videos, they identified different type of behaviours, including close approaches to nacelle and monopole, close approaches to slowly moving blades, flight loops and dives centred at the turbine, distant hovering and chasing other bats toward or near the turbines. Twelve bat fatalities were recorded under turbines after the camera-nights. Focal bat behaviours, including close approaches to the monopole (13%), nacelle (30%) and occasionally blades (6%), were observed for wind speeds ranging from 0 to 9.60 m/s. They suggested that bats are observed more frequently at lower wind speeds and most fatalities occur during late summer and autumn at average wind speed of 5–6 m/s. Arnett et al[24] also mentioned that bat fatalities are highest on nights with low wind speeds less than 6 m/s.

The ballistics model proposed by HM10[20] estimates a 1-D fall zone distributions of bat carcasses, radially away from the turbine base, whereas Biswas et al[21] and Sarlak and Sørensen[22] can produce 2-D fall zone distributions of ice fragments and broken blade fragments, respectively. To explore the use of ballistics models to describe bat carcass fall zones around wind turbines, the following hypotheses are proposed and investigated:

1. Wind significantly effects the trajectory of a bat carcass after strike by turbine blade
2. Uncertainty of bat biophysical and aerodynamic characteristics, meteorological conditions, turbine model and operation, and bat flight trajectory prior to blade strike affect a carcass fall trajectory

3. Bat strike locations on a turbine rotor can be estimated using a ballistics model, guided by carcass survey and supervisory control and data acquisition (SCADA) records

This paper proposes a new bat carcass ballistics modelling framework that includes wind drift, coefficient of restitution, bat flight speed, and bat strike angle, and investigates the influence of input parameters on the distribution of ground impact patterns. The model is also used to demonstrate how to calculate the likely strike location on the rotor to provide insights on bat–turbine interaction.

2 | STUDIED WIND FARM

In this study, we utilize the data collected at a wind farm in central Iowa, USA. The wind plant consists of 51-Siemens SWT-2.3 MW wind turbines. The radius (R) of the turbine rotors is 54 m, the turbine hub height (H_{hub}) is 80 m and the rotor swept area is 9,160 m^2 per turbine. The turbine SCADA contains records of meteorological data (e.g., wind speed) and turbine operational parameters [e.g., yaw and rotation rate (RPM)], which are input parameters for the ballistics model. Yaw is defined as the direction the turbine faces relative to North. A wind speed versus RPM relationship was developed from SCADA data by analysing records from the SCADA for the wind turbines.[25] The carcass survey data were collected by biologists to estimate the total number of fatalities at the wind farm. The survey data report carcass species, date found, estimated time since death, carcass coordinates and carcass condition (e.g., intact or scavenged).

Figure 1 illustrates the front-view (xz-plane), side-view (yz-plane) and plan-view (xy-plane) of a turbine and trajectory of a falling carcass showing the displacement carcass distance, including the carcass in-plane distance from turbine base and carcass normal distance from the rotor plane. In Figure 1A, r indicates the carcass radial position vector, measured from the hub and θ denotes the carcass angular position vector measured from horizontal, in the positive x-direction, and increasing in the anti-clockwise direction. In Figure 1B, ψ shows the angle at which bats impact the turbine blades. It is referenced relative to the rotor plane and is positive in downwind direction and negative in upwind direction. Figure 1C shows the plan-view perspective and defines the distance the bat carcass falls from the turbine including the total distance from the tower ('Carcass distance'), distance from the tower within the rotor plane ('Carcass in-plane distance') and distance from the rotor plane ('Carcass normal distance').

3 | ASSESSING THE EFFECT OF WIND DRIFT ON FALLING CARCASSES

To determine if bat carcasses fall primarily within the rotor plane after the collision can be tested by plotting the rotor plane and computing carcass normal distance from the rotor plane. This requires the turbine yaw angle for determining rotor plane location at the time of collision and

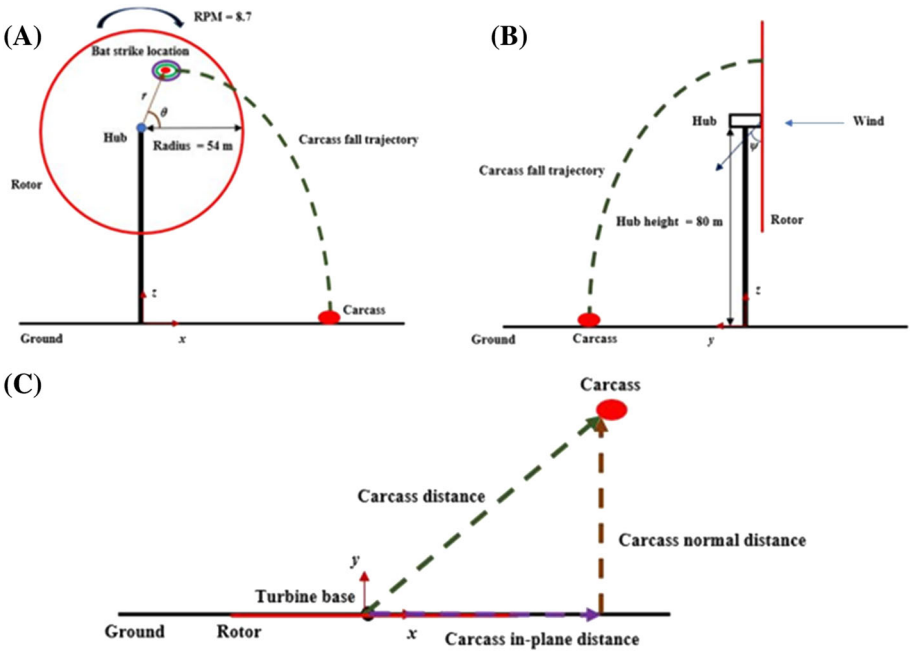

FIGURE 1 Schematic of bat strike and carcass trajectory. (A) Front view, (B) side view and (C) plan view

carcass distance and bearing for computing carcass normal distance relative to the rotor plane. The collision between bat and turbine blades is an instantaneous phenomenon. However, survey data can only provide information about the night a collision occurs. Therefore, it is not possible to quantify yaw or rotor plane orientation at the moment of collision. Also, rotor plane orientation varies depending upon the wind direction and as a result adds uncertainty to the carcass landing position. Only carcases surveyed as died on the previous night were investigated to evaluate if a carcass landed within the rotor plane or drifted due to the wind.

The carcass survey and SCADA data from 2018 are used in this study. The carcass survey data for the 2018 Fall migration period (15th July to 13th October) reported a total of 261 bat carcasses. For computing the rotor plane location with confidence, bat mortalities that reported 'last night' as the 'estimated time of death' in the carcass survey data, were selected. These fresh carcasses have smaller time interval to evaluate the meteorological and turbine operational conditions and as a result minimize the uncertainty of yaw (turbine orientation). For 'last night' fatalities, yaw from 8 pm (of the previous day when carcass was found) to 5 am (of the day when the carcass was found) is analysed to investigate its variation with time. The mean and standard deviation of yaw time series for the selected period was calculated. Supporting the selected period of analysis, Cryan et al[23] reported that bats are generally more active from dusk to dawn. The 'last night' fatalities in which standard deviation of yaw was ≤15° were selected since the rotor plane can be described with limited uncertainty. For these 'last night invariant yaw' fatalities, the rotor plane and consequently the carcass location relative to the rotor can be determined with high confidence to compute the carcass normal distance from the rotor plane. Out of the 261 carcasses discovered in the wind farm, 80 bat fatalities were identified as 'last night' fatalities. On analysing the yaw data of the 'last night' fatalities for the time window of 8 pm (of the previous day of carcass discovery) to 5 am (of the day of carcass discovery), it was found that 29 of the 'last night' fatalities satisfied the yaw invariance criterion. After establishing the rotor plane for the 'last night invariant yaw' fatalities, the carcass normal distance with respect to the rotor plane was computed. It was found that finally 16 bat fatalities satisfied the condition of 'last night invariant yaw with carcass normal distance > 10 m'. The bat species identified in these cases were the hoary bat, the eastern red bat and the silver-haired bat. It is important to recognize that the above-mentioned constraints resulted in a limited number of bat fatalities investigated and consequently the results and conclusions of this study are therefore limited.

To evaluate the effect of wind drift, SCADA data including wind speed and turbine operational conditions were analysed for one of the eastern red bat fatalities found on 21 August 2018. Using the yaw data, the orientation of the turbine as well as the carcass survey location with respect to the turbine base is determined. Survey data reported the carcass distance was 45 m from the base of the turbine at a bearing of 210°. Figure 2A displays the time series plot of RPM, yaw and wind speed from 8 pm on 20 August to 5 am on 21 August. The mean and standard deviation of yaw were 0° and 11°, respectively. The carcass in-plane (from turbine base in *xz*-plane) and normal distance (from rotor plane in *xy*-plane) was computed as 22 and 39 m, respectively. The solid line and dashed line in Figure 2B represent the average orientation of the rotor plane and the standard deviation. The cross (x) in the plan-view represents the surveyed carcass location whereas the rotor plane faces towards the North direction, indicated by a unit normal vector shown at the centre of the rotor. All of the cases satisfying the criterion of 'last night invariant yaw fatalities with carcass normal distance > 10 m' were investigated (see Data S1). The evidence from these fatalities indicate that carcasses land downwind of the wind turbine at significant distances outside of the rotor plane, that is, outside of turbine pad at the distance of 1.5–2 times of the turbine pad diameter. The likely cause of carcasses falling downwind of the rotor is wind drift. Therefore, a model describing where carcasses fall needs to account for the effects of wind drift.

4 | CARCASS BALLISTICS MODEL WITH WIND DRIFT

A ballistics model with three degrees of freedom was proposed to incorporate the plausible parameters leading to 3-D carcass fall trajectory as observed in Figure 2B. One of the purposes of the present study is to determine how the range of different input parameters in the model affects the carcass 3-D fall trajectory and strike distribution on the rotor plane. After striking a turbine blade, bats are assumed to be passive particles that can no longer fly. Therefore, aerodynamic drag and gravitational force (i.e., carcass weight) are the forces acting on the falling carcass. Given an initial velocity, a 3-D ballistics model can represent a bat carcass as a ballistics particle falling until the carcass reaches the ground. The governing equations of the 3-D ballistics model describing the carcass velocity and position are as follows:

$$\frac{d^2x_c}{dt^2} = -\frac{\rho}{2}\left(\frac{C_d A_c}{m_c}\right)\left(\frac{dx_c}{dt}\right)|V_c| \tag{1}$$

$$\frac{d^2y_c}{dt^2} = -\frac{\rho}{2}\left(\frac{C_d A_c}{m_c}\right)\left(\frac{dy_c}{dt} - W_s\right)|V_c| \tag{2}$$

$$\frac{d^2z_c}{dt^2} = -\frac{\rho}{2}\left(\frac{C_d A_c}{m_c}\right)\left(\frac{dz_c}{dt}\right)|V_c| - g \tag{3}$$

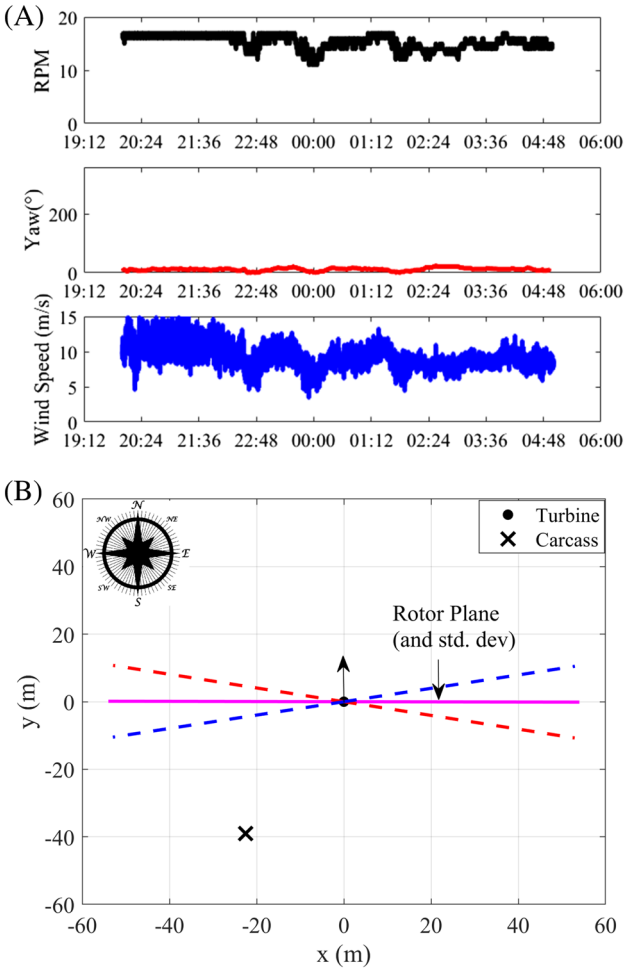

FIGURE 2 (A) SCADA data records for a night when the eastern red bat was killed. (B) Plan-view of turbine orientation and carcass survey (the direction icon is procured from creative commons, https://search.creativecommons.org/photos/5ac90cd2-c4b6-4e85-9a96-3e9bfa9a96f5)

$$|V_c| = \sqrt{\left(\frac{dx_c}{dt}\right)^2 + \left(\frac{dy_c}{dt} - W_s\right)^2 + \left(\frac{dz_c}{dt}\right)^2} \tag{4}$$

where m_c is the carcass mass; A_c is the carcass projected area; C_d is the carcass drag coefficient; W_s is the wind speed in the y-direction; ρ is the air density; g is the gravitational acceleration in the z-direction and x_c, y_c and z_c are the components of carcass position vector relative to the ground in the x-, y- and z-directions, respectively. The ratio of aerodynamic drag (C_dA_c) and mass (m_c), as introduced in Biswas et al[21] for ice fragments, is a suitable parameter to examine the relative effect of bat biophysical and aerodynamic characteristics. The parameters were combined to form a lumped carcass parameter (C_dA_c/m_c), which is useful for exploring the sensitivity of carcass fall trajectory with respect to the properties of bats. The system of differential equations can be solved numerically using a fourth-order Runge–Kutta method. The following assumptions are made:

1. Simulations are performed for constant wind in a direction normal relative to the rotor plane, and therefore W_s (x, y, z) = Constant
2. Carcasses bodies are compact after blade strike and lift forces on a bat carcass are considered to be negligible
3. Carcasses do not bounce upon impact with the ground

The initial velocity of the carcass at the moment of contact with the turbine blade is dominated by the velocity of the blade. The initial position and velocity of the bat carcass at t = 0 are ($r\cos\theta$, 0, H_{hub} + $r\sin\theta$) and (($1 + e$)$r\omega\cos\psi\sin(90^\circ\text{-}\psi)\sin\theta$, V_{bat} + ($1 + e$)$r\omega\cos\psi\cos(90^\circ\text{-}\psi)$, –($1 + e$)$r\omega$ $\cos\psi\sin(90^\circ\text{-}\psi)\cos\theta$), respectively. V_{bat} is the bat flight speed normal to the rotor plane prior to strike. The coefficient of restitution e determines the initial velocity of a carcass after blade strike. It is a physical parameter that describes the ratio of relative velocity between the bat and turbine blade before and after a collision. The value varies between 0 and 1, with 0 representing an inelastic collision where the carcass assumes the local blade velocity, and 1 representing a fully elastic collision where the carcass velocity is twice the blade velocity.

The estimation of carcass trajectory requires accurate description of carcass' aerodynamics; in particular, an estimate of drag coefficient is required. Prakash and Markfort[26] reported the first measurements of bat carcass drag coefficients. Drag coefficients were determined for three bat species (hoary bat, eastern red bat and evening bat) and were found to be within a range of 0.70–1.23, with corresponding terminal velocity between 6.6 and 17.6 m/s.

5 | SENSITIVITY OF CARCASS BALLISTICS TRAJECTORIES TO INPUT PARAMETERS

Bat carcass fall trajectories and final impact positions on the ground are dependent on the input parameters of the ballistics model, which can be classified into the following five categories: (1) carcass strike location on the rotor plane described by a radial (r) and angular position (θ), (2) bat biophysical and aerodynamic properties represented by the carcass parameter (C_dA_c/m_c), (3) meteorological and turbine operational conditions (wind speed and RPM), (4) collision dynamics describing the initial velocity of the carcass represented by coefficient of restitution (e), and (5) bat flight characterisitcs of bat flight speed (V_{bat}) and bat strike angle (ψ). The biophysical and aerodynamic characteristics of the hoary bat (heaviest) and the evening bat (lightest) discovered in the field campaign reported in Prakash and Markfort[26] were selected for the sensitivity analysis. It is therefore important to reiterate here that the sensitivity analysis results are based on the limited sampling of three freshly discovered bat carcasses. The corresponding carcass parameter for hoary bat was 0.05 m^2/kg and for evening bat was 0.30 m^2/kg. A typical wind speed of 5 m/s and a corresponding turbine rotor RPM of 8.7 was selected as turbines are curtailed below wind speed of 5 m/s and bats are most active at lower wind speeds. The turbine geometry was selected based on the Siemens-2.3 MW wind turbine described in Section 2.

5.1 | Effect of carcass' blade strike location on the rotor plane

Carcass strike location on the rotor plane and rotor rotation rate governs the initial velocity of the turbine blade, which determines the initial velocity of the carcass. Figure 3A,B shows the plan-view (xy-plane) of the numerical solution of the ballistics model for carcass impact positions on the ground ($z = 0$) with varying initial radial and angular positions for the hoary bat and the evening bat, respectively. Note, the turbine is located at the origin ($x = 0$, $y = 0$). For the hoary bat, the maximum total distance was estimated as 93 m for $r = 54$ m and $\theta = 220^\circ$, whereas for the evening bat, the maximum total distance was 99 m for $r = 54$ m and $\theta = 95^\circ$. From carcass survey data, the hoary bats were found to fall up to 51 m from tower, whereas the evening bats were observed to land to maximum distance of 40 m from tower, highlighting that the carcasses fall well within the modelled maximum distances. Based on the computations of Figure 3, it is evident that different strike position on the rotor plane results in significant differences in the ground impact location of carcasses.

5.2 | Effect of carcass parameter (C_dA_c/m_c)

The ballistics model described by Equations 1, 2 and 3 consists of the aerodynamic drag and gravitational force. The aerodynamic characteristic is represented by a lumped parameter, (C_dA_c), whereas the gravitational force is dependent on m_c. A carcass parameter (C_dA_c/m_c) was defined to investigate the relative effect of aerodynamic drag and inertia on carcass fall trajectories. Figure 4 shows the plan-view of distributions of impacts on the ground obtained from the modelled bat trajectories on the rotor tip, at different angular positions on the rotor under different operating conditions. Six values of carcass parameter were selected for the sensitivity analysis: 0.05, 0.10, 0.15, 0.20, 0.25 and 0.30. It should be noted that (C_dA_c/m_c) = 0.05 m^2/kg corresponds to the hoary bat, whereas (C_dA_c/m_c) = 0.30 m^2/kg corresponds to the evening bat. It was found that with increased (C_dA_c/m_c), the carcass in-plane distance decreases, whereas the carcass normal distance increases. The results shown in Figure 4 illustrate that bats with a larger carcass parameter (e.g., the evening bat) experience relatively larger wind drift due to the dominant effect of aerodynamic drag, whereas bats with a smaller carcass parameter (e.g., the hoary bat) have larger in-plane distances due to significant inertia resulting from blade strike.

5.3 | Effect of wind speed and rotor RPM

The rotor rotation rate (RPM) of wind turbines is an important parameter in the ballistics model for determining the carcass impact locations on the ground. The RPM is directly related to wind speed. Higher wind speed leads to larger RPM, which in turn imparts larger initial velocity to carcasses. Figure 5A,B displays the wind speed versus RPM effect on the carcass ground impact patterns for the hoary bat and the evening bat, respectively. Two wind speeds of 5 and 10 m/s were considered which yields the RPM value of 8.7 and 17.2, respectively. From Figure 5, it is evident that for the hoary bat, the increment in wind speed/RPM affects both the in-plane and downwind distance of carcasses. On the other hand,

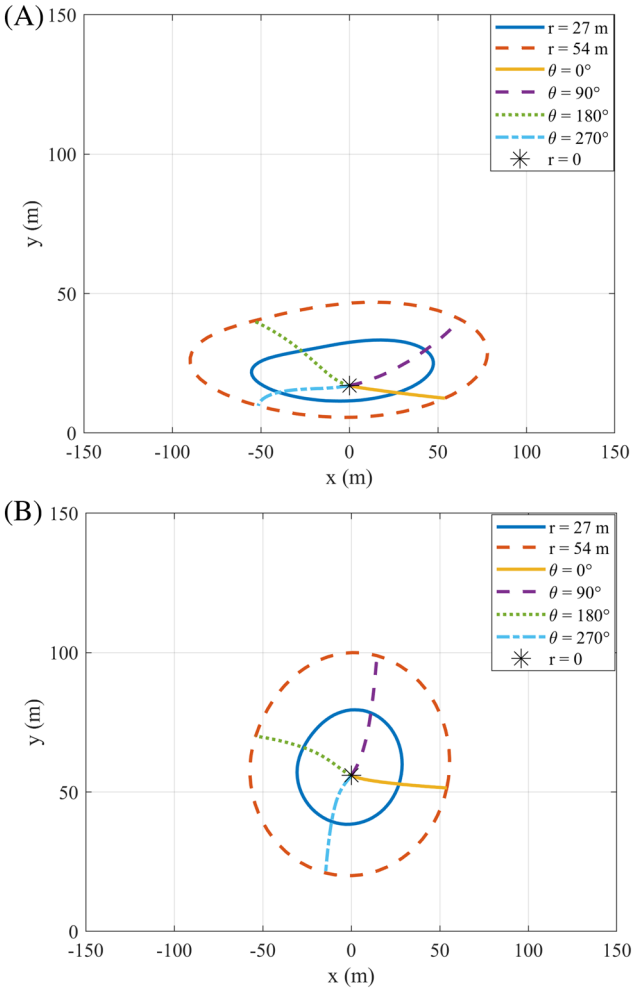

FIGURE 3 Plan-view of carcass ground impact pattern for blade strikes at different radial and angular positions, (A) $(C_dA_c/m_c)_{hoary}$ = 0.05 m^2/kg and (B) $(C_dA_c/m_c)_{evening}$ = 0.30 m^2/kg (W_s = 5 m/s, RPM = 8.7, e = 0, V_{bat} = 0 and ψ = 0. Note, the turbine is located at the origin, that is, x = 0, y = 0)

for the evening bat, the increase in wind speed and RPM influence primarily the downwind distances behind the rotor plane. The effect of wind speed/RPM is much more evident on downwind distances as compared to the in-plane distances.

5.4 | Effect of coefficient of restitution (*e*)

The magnitude of the initial velocity imparted to the bat carcass is determined by the blade velocity and the coefficient of restitution. It accounts for the collision type between the turbine blade and bat and incorporates many factors such as bat orientation and contact time at the time of blade strike. The value of e lies between 0 (fully inelastic collision) and 1 (fully elastic collision). Figure 6A,B shows the plan-view of carcass ground impact pattern for e = 0 and 1 for the hoary bat and the evening bat, respectively. It is evident from Figure 6 that for the hoary bat, extreme variation of e from minimum to maximum results in larger in-plane distance and wind drift showing a strong influence of initial impact velocity on carcass ground impact pattern. Conversely for the evening bat, it was found that e variation does not have a significant influence on carcass ground impact pattern. Previously performed experiments on freshly discovered (never frozen) bat carcasses, reported in Martin et al,[25] found $e \approx 0.1$ with little variation between bat species.

5.5 | Effect of turbine models (GE-1.5 MW vs. Siemens-2.3 MW)

In order to investigate the effect of different wind turbine models, the fall zone distributions of bat carcasses were compared for two wind turbines, GE-1.5 and Siemens-2.3 MW. The hub height was held constant at 80 m for both turbines, whereas the rotor radius was 35.5 m and 54 m for GE-1.5 and Siemens-2.3 MW, respectively. The simulations were performed for both turbines corresponding to the operating conditions associated with the wind speed of 5 m/s. This results in rotor RPMs of 12 and 8.7 for the GE-1.5 and Siemens-2.3 MW turbines,

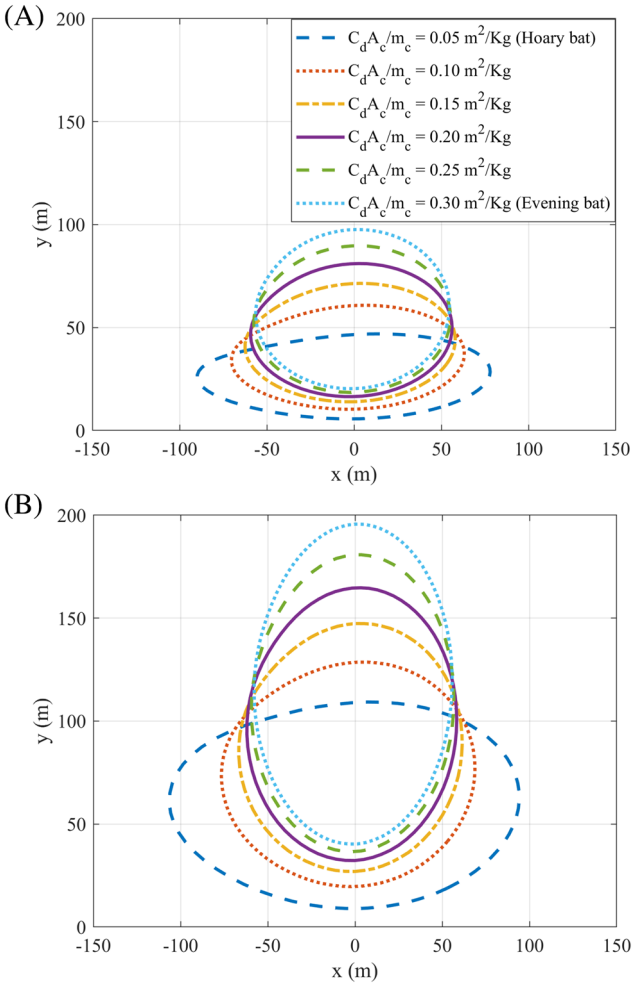

FIGURE 4 Plan-view of carcass ground impact pattern with carcass parameter variation, (A) W_s = 5 m/s, RPM = 8.7 and (B) W_s = 10 m/s, RPM = 17.2 (r = 54 m, e = 0, V_{bat} = 0 and ψ = 0)

respectively. Fall zone distributions of the hoary bat (Figure 7A) and the evening bat (Figure 7B) were generated for the two turbine specifications, assuming fully inelastic collision (e = 0). Generally, the impact pattern covers an overall larger area for both species of bat striking the larger wind turbine. It is evident from Figure 7 that the longer rotor blades influence the impact pattern more than increased rotation rate, as the impact pattern is a larger area for the larger but slower Siemens turbine than the smaller but faster GE turbine. The hoary bat carcass travelled a maximum of approximately twice the blade length in the x-direction for the GE wind turbine, while only approximately one and a half times the blade length for the Siemens turbine. The lighter evening bat travelled furthest in the downwind direction (y-direction), approximately 70% of the turbine total height for both wind turbines. Since the Siemens wind turbine is nearly 20 m taller than the GE, the carcass travelled nearly 20 m further downwind.

5.6 | Effect of bat flight speed (prior to strike)

Bat flight speed prior to the collision might play an important role in governing the carcass ground impact patterns. As a result, we considered the flight speed of bats prior to strike and estimated the ground impact patterns of both the hoary bat and the evening bat carcasses. Hayward and Davis[27] found the flight speed of the big brown bats as 2–7 m/s, whereas McCracken et al[28] measured the median flight speed of the Brazilian free-tailed bats as 5.7 m/s. Martin et al[25] reported the flight speed of species of concern in the Midwestern region as ~5–10 m/s. Based on these findings, in the present analysis, three flight speeds of 0, 5 and 10 m/s (relative to the rotor) were considered for the sensitivity analysis, both along the wind (positive y-direction) and opposite the wind (negative y-direction). Figure 8 shows the ground impact pattern of the two bat species obtained after incorporating the bat flight speed (prior to the strike) in the proposed ballistics model.

It can be seen from Figure 8A that as the hoary bat flight speed is increased from 0 to 5 m/s (along the wind), the maximum downwind distance increased from 47 to 54 m, whereas when the bat flight speed is increased from 0 to 10 m/s, the maximum downwind distance increased

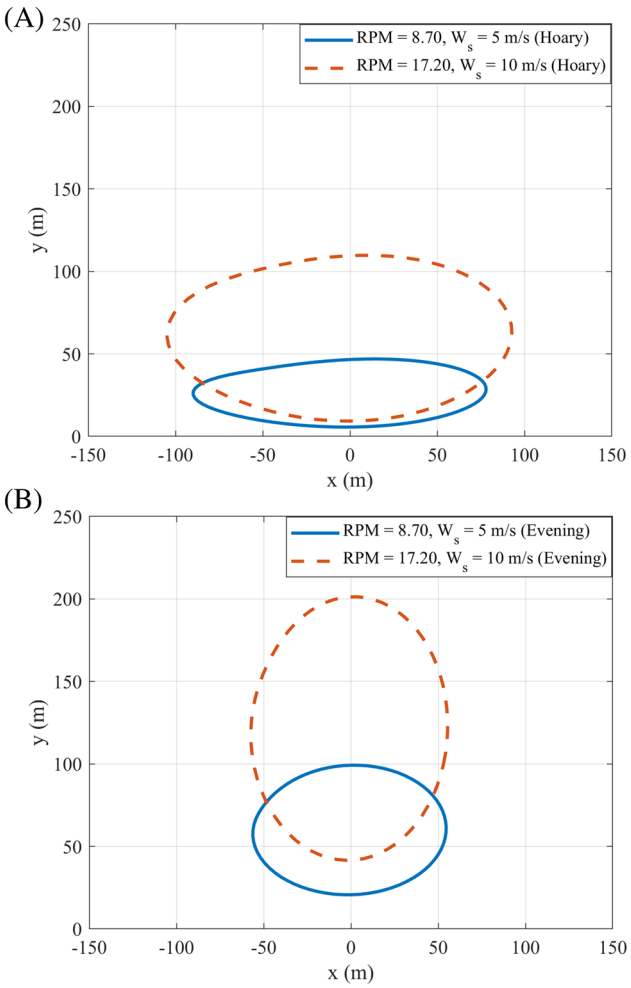

FIGURE 5 Plan-view of carcass ground impact pattern with wind speed versus RPM relationship variation, (A) $(C_dA_c/m_c)_{hoary}$ = 0.05 m^2/kg and (B) $(C_dA_c/m_c)_{evening}$ = 0.30 m^2/kg (r = 54 m, e = 0, V_{bat} = 0 and ψ = 0)

by 16 to 63 m, although the in-plane distance is not significantly affected in both cases. When the bats move opposite to the wind, the ground impact patterns were found to shift towards the rotor plane with few trajectories resulting in carcasses landing slightly upwind of the rotor for 10-m/s case.

For the evening bat (Figure 8B), the influence of flight speed prior to strike does not affect either the in-plane or the downwind distances significantly, indicating the wind drift to be the dominant factor in determining the bat ground impact patterns. Based on these results, it can be concluded that bat flight speed plays an important role in governing the fall trajectories of bats with smaller carcass parameter.

5.7 | Effect of bat strike angle

The angle that a bat strikes the turbine blade has significant uncertainty due to blade curvature and blade pitch angle, and it may be significant in affecting carcass fall trajectories. We investigated the effect of bat strike angle on the sensitivity of carcass ground impact patterns for strike angles ψ = 0°, ±45° and ±90°. Figure 9 shows the carcass ground impact patterns of five strike angles for the hoary bat and the evening bat. The wind speed and bat flight speed in these simulations were set at 5 m/s and 0, respectively.

It should be noted here that a strike angle of 0° corresponds to a direct bat-blade strike whereas for a ±90° strike angle, the bat experiences a glancing strike, resulting in mortality but not significant kinetic energy transfer such that bats experience only wind drift causing the carcasses to land behind the rotor plane. For the hoary bat, a strike angle of 0° results in a maximum in-plane distance of 89 m and maximum downwind distance of 47 m (Figure 9A). The strike angle of ±90° results in both shorter maximum in-plane (53 m) and downwind distance (32 m). For ±45° bat strike angle, the kinetic energy transfer from blade to bats occurs equally in both rotor plane (xz-plane) and rotor normal direction (±y-axis). The bat strike angle of +45° yields maximum downwind distance of 85 m, 36 m further downwind. The maximum in-plane distance is reduced with respect to 0° case by 22 m. However, for −45° strike angle, the bats fall in front of the rotor with maximum upwind distance of 20 m. For both species, both in-plane and normal maximum distances were computed for carcasses situated at r = 54 m and θ = 0°, 90°, 180°, and 270°, for

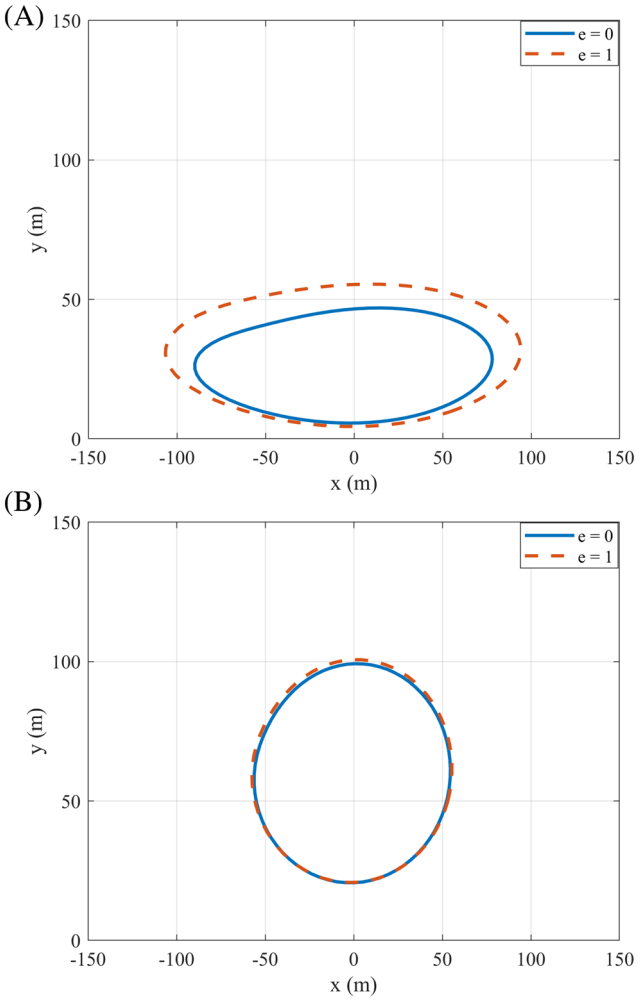

FIGURE 6 Plan-view of carcass ground impact pattern with coefficient of restitution variation, (A) $(C_d A_c/m_c)_{hoary}$ = 0.05 m^2/kg and (B) $(C_d A_c/m_c)_{evening}$ = 0.30 m^2/kg (W_s = 5 m/s, RPM = 8.7, r = 54 m, V_{bat} = 0 and ψ = 0)

different values of ψ (−90° to 90°, see details in the supporting information). The results revealed that for $\psi \sim 40°–60°$, the carcass attains the maximum normal distance for both species.

For the evening bat in Figure 9B, it can be seen that for the five strike angles, the difference in carcass normal distance is approximately 18 m, whereas the in-plane distance remains the same indicating that the fall dynamics for the evening bat is primarily governed by wind drift. Based on these results, we can infer that for a 5-m/s wind speed, the fall trajectories of bats with smaller carcass parameter are significantly affected by bat strike angle.

6 | ESTIMATING BAT STRIKE LOCATION ON THE ROTOR BASED ON CARCASS SURVEY AND SCADA DATA

Bats flying around wind turbines have been found to exhibit behaviour patterns that may be useful for designing technologies to avoid blade strike (Cryan et al[23]). However, it remains poorly understood if bats are more likely to be hit within a specific region of the rotor. Using carcass surveys and SCADA information, the new ballistics model can be used to backtrack from the location a carcass found on the ground to where it was likely struck by the turbine blade. Considering selected cases of carcasses found in the 2018 survey for the Iowa wind farm, the following provides detailed investigation performed to demonstrate the model as a tool to determine the distribution of strike locations on the rotor plane.

6.1 | Carcass survey and associated SCADA details for selected bat fatalities

The 'last night invariant yaw fatalities, with carcass normal distance > 10 m' of the hoary bat and the eastern red bat were selected for computing the likely strike locations of bats on the rotor plane. The description of these fatalities including date the carcass discovered, species, distance and

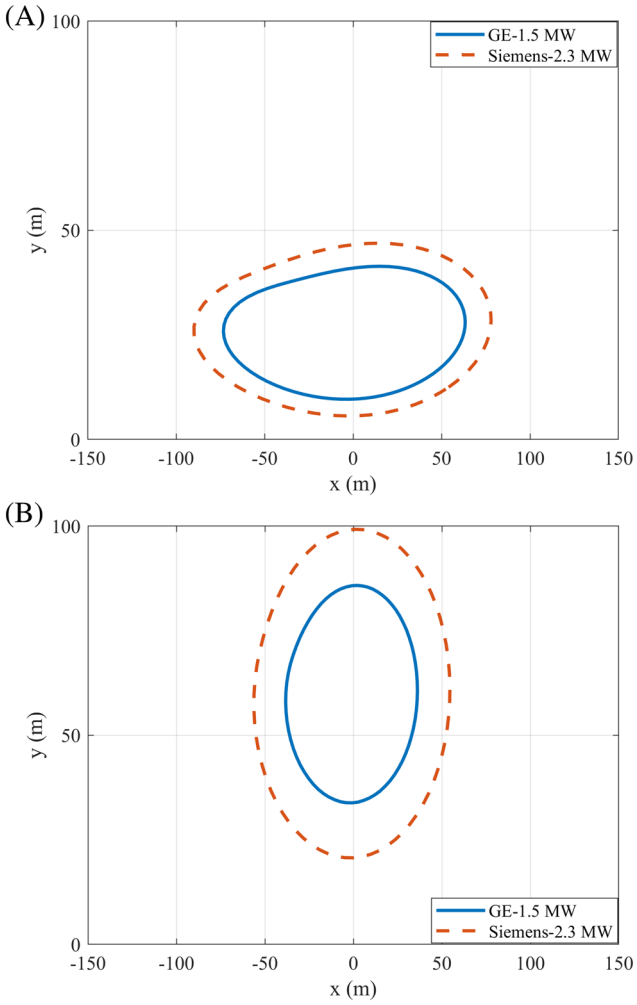

FIGURE 7 Plan-view of carcass ground impact pattern with turbine model variation, (A) $(C_dA_c/m_c)_{hoary}$ = 0.05 m^2/kg and (B) $(C_dA_c/m_c)_{evening}$ = 0.30 m^2/kg (e = 0, V_{bat} = 0 and ψ = 0)

bearing from the turbine, wind speed and RPM, and mean yaw for a specified window of 8 pm (of the previous day when carcass was found) to 5 am (of the day when the carcass was found). A summary of data for seven cases, where yaw, RPM, wind speed is known, is presented in Table 1. The carcass' bearing and yaw were measured from North in clockwise direction. The details of Table 1 were used as input in the ballistics model to identify the plausible strike locations of bats on the rotor. Aerodynamic properties are assumed based on the findings in Prakash and Markfort.[26]

6.2 | Parameter matrix for computing ensembled ground impact distribution

The survey data do not provide details for mass and projected area for the bat carcasses. Therefore, mass and projected area were approximated based on survey records collected over multiple seasons and provided in support of a Habitat Conservation Plan (HCP) for Iowa wind energy.[29] To support the range of values, additional biological references[30,31] were also considered. The range of bat mass, projected area (derived based on forearm length) and drag coefficient of the hoary bat and the eastern red bat is listed in Table 2. Another source of uncertainty stems from the coefficient of restitution. The range of 0–0.1 was selected based on experiments performed using fresh carcasses (Martin et al[25]).

A parameter matrix was proposed to run the simulations for a range of bat carcass parameter (C_dA_c/m_c), wind speed (W_s), turbine operation (RPM) and coefficient of restitution (e). The criterion for defining the combinations of the parameters was as follows: (a) lower bound (LB), mean and upper bound (UB) of wind speed time series, which is proportional to the LB, mean, and UB of the rotor RPM time series, respectively, and (b) heavier bats have large projected areas. On the basis of these two conditions, each of the three W_s versus RPM pair was coupled with $(C_dA_c/m_c)_{min}$, $(C_dA_c/m_c)_{mean}$ and $(C_dA_c/m_c)_{max}$ to yield a total of nine combinations to run the model. Table 3 reports the nine combinations of the parameter matrix of the eastern red bat fatality shown in Figure 2, only for e = 0.

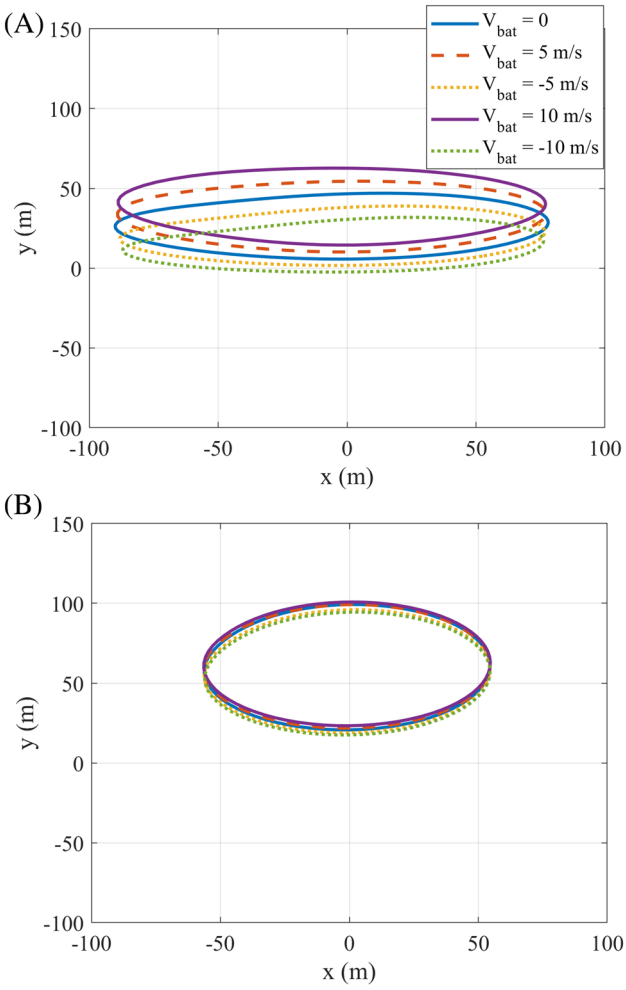

FIGURE 8 Plan-view of carcass ground impact pattern with bat flight speed, (A) $(C_dA_c/m_c)_{hoary}$ = 0.05 m^2/kg and (B) $(C_dA_c/m_c)_{evening}$ = 0.30 m^2/kg (W_s = 5 m/s, RPM = 8.7, e = 0 and ψ = 0)

The resulting fall zone distribution for the nine simulations, which are repeated for two values of e, produces a total of 18 fall zone distributions. These were linearly combined to generate an ensemble fall zone distribution. Using the resulting distribution, trajectories were analysed for the carcases nearest to the surveyed carcass. These were backtracked to identify its probable strike location on the rotor, at the time of collision.

6.3 | Bat strike location estimation methodology

The location of the surveyed bat carcasses discovered on the ground after the blade strike is the result of numerous factors including bat biophysical and aerodynamic properties, wind speed, turbine operational characteristics, collision dynamics, bat flight trajectory, and bat strike location on rotor. The following is the step-by-step procedure followed for estimating the likely bat strike location on the wind turbine rotor where a bat most likely hits the turbine rotating blade.

1. For a surveyed bat fatality, bats distributed on the rotor plane at a radial resolution of 1 m and angular resolution of 5° were considered, leading to a simulation of 3,960 bats.
2. Run the ballistics model for stationary bats on the rotor plane with e = 0 and, with the corresponding wind speed and RPM for the nine combinations described in Table 3. This results in nine fall zone distributions for the bat fatality. Combine the nine distributions to compute the ensembled fall zone distribution for a bat fatality with e = 0.
3. Repeat Steps 1 and 2 for e = 0.1 to generate another ensembled fall zone distribution of the fatality.
4. Combine the two ensembled distributions (for e = 0 and 0.1) to generate a final ensembled 2-D fall zone distribution of the selected bat fatality.
5. Superimpose the carcass survey position (with respect to turbine) on the final ensembled 2-D fall zone distribution and choose a square window of 10 × 10 m around the carcass to account for the uncertainty in the recorded carcass survey location.

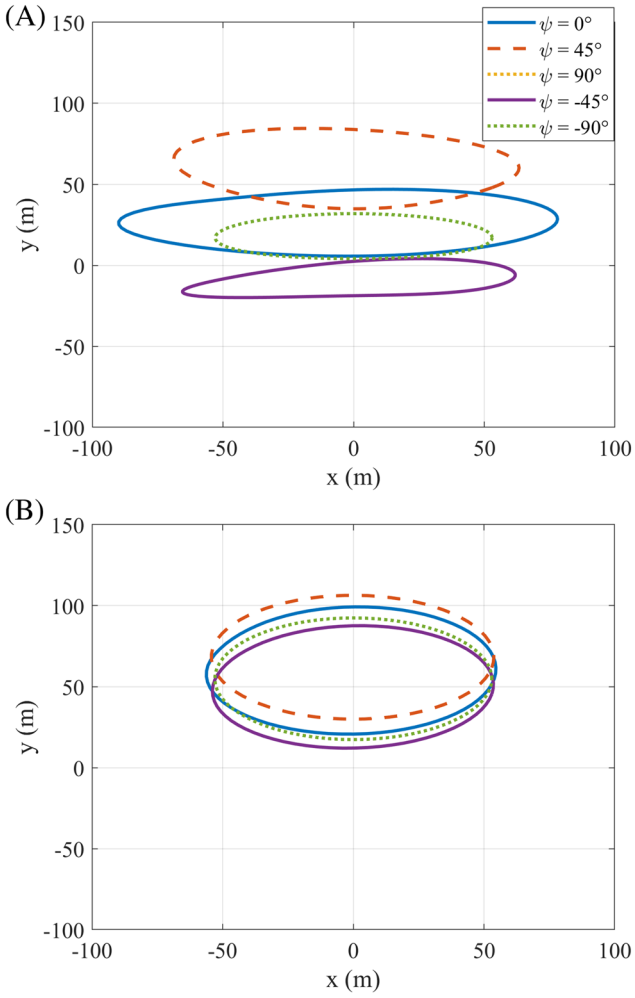

FIGURE 9 Plan-view of carcass ground impact pattern with bat strike angle, (A) $(C_dA_c/m_c)_{hoary}$ = 0.05 m^2/kg and (B) $(C_dA_c/m_c)_{evening}$ = 0.30 m^2/kg (W_s = 5 m/s, RPM = 8.7, e = 0, V_{bat} = 0)

TABLE 1 Bat fatality details

Carcass search date	Species	Distance from turbine (m)	Bearing from turbine (°)	Wind speed range	RPM range	Mean yaw	Carcass in-plane distance (m)	Carcass normal distance (m)
09/08/2018	Hoary	39	199	6.7 ± 1.0	12.0 ± 1.2	46°	18	35
09/08/2018	Hoary	46	240	5.4 ± 1.5	10.7 ± 1.6	50°	9	45
09/08/2018	Hoary	48	220	7.6 ± 1.0	13.3 ± 1.1	43°	0	48
08/21/2018	Eastern red	45	210	9.4 ± 1.8	15.6 ± 1.3	0°	22	39
09/14/2018	Eastern red	36	282	8.3 ± 0.6	14.2 ± 0.9	176°	35	10
09/17/2018	Eastern red	31	6	9.2 ± 1.2	14.5 ± 1.2	185°	0	31
09/25/2018	Eastern red	34	3	7.0 ± 1.3	12.8 ± 1.4	204°	12	32

6. Locate the simulated bat carcasses in the identified window from the solution of the ballistics model. This provides the pool of possible candidates from bats on the rotor plane which fell around the carcass location reported in the survey data.
7. Backtrack these carcasses to identify the radial and angular position (r, θ) of the bats to determine the approximate bat strike location on the rotor plane.

TABLE 2 Range of bat carcass mass, projected area and drag coefficient

Bat carcass properties	Range	
	Hoary bat	Eastern red bat
Mass (m_c)[29–31]	18–38 g	9–17 g
Projected area (A_c)[29–31]	10–23 cm^2	8–17 cm^2
Drag coefficient (C_d)[26]	0.70–0.73	0.74–0.80
Coefficient of restitution (e)[25]	0–0.1	

TABLE 3 Parameter matrix for ensembled distribution of the eastern red bat (e = 0)

Combination #	W_s (m/s) & RPM	C_dA_c/m_c (m^2/kg)
C1	W_s = 7.6 m/s RPM = 14.3	0.06
C2		0.07
C3		0.08
C4	W_s = 9.4 m/s RPM = 15.6	0.06
C5		0.07
C6		0.08
C7	W_s = 11.2 m/s RPM = 16.7	0.06
C8		0.07
C9		0.08

8. For the identified region of particles approximating the bat strike location on the rotor, run the ballistic model with higher resolution within that region to generate a 2-D fall zone distribution of bats. Then identify the carcasses landing in the refined window of 5 × 5 m around the carcass survey location.
9. Repeat Step 5 to identify the bat carcasses landing in the marked window to determine the bat strike location cumulative frequency contours on the rotor plane.
10. Identify the location with highest strike probability on the rotor. Compute carcass back-trajectory from the ballistics model, struck by the blade at the identified probable location on the rotor. Cross check the accuracy of the 3-D ballistics model results by comparing the carcass modelled total distance (from turbine base) to the observed total distance.

6.4 | Bat strike location results

The bat strike location estimation methodology presented in Section 6.3 was implemented for bat fatalities reported in Table 1. The bat strike location results are computed assuming zero bat flight speed (V_{bat} = 0) and zero bat strike angle (ψ = 0) due to the significant uncertainties associated with these parameters. Further investigations could consider using thermal video recordings to estimate pre-strike flight speed and angle. As an illustration of the estimation procedure, only the results for one of the eastern red bat fatalities are shown with the results of other cases presented in the supporting information. The SCADA data record for the night when the bat fatality occurred and plan-view of the location of ground impact with respect to turbine are shown in Figure 2. First, the ballistics model was run for the nine combinations in Table 3. It incorporates the uncertainty in the bat biophysical and aerodynamic properties, meteorological features and corresponding turbine operational conditions, for e = 0. Figure 10 shows the 2-D fall zone distribution of the nine combinations of the parameter matrix.

The black dot at the origin along with the thick black line shows the turbine base and rotor plane. Wind, uniform in the vertical direction, was assumed to be aligned normal to the rotor plane. Along the horizontal direction (from left to right, C1 → C3, C4 → C6 and C7 → C9) in Figure 10, the carcass parameter (C_dA_c/m_c) increases for the same W_s versus RPM relation whereas in the vertical direction (from top to bottom, C1 → C7, C2 → C8 and C3 → C9), W_s versus RPM values increases for a constant (C_dA_c/m_c). It was observed that the hotspot of highest probability of carcass landing positions shifts further away from the turbine for higher wind speeds. It indicates that fall distances travelled by bat carcasses behind the rotor plane increased with W_s versus RPM magnitude.

The nine fall zone distributions in Figure 10 for e = 0 were combined to yield an ensembled fall distribution for the eastern red bat. The same procedure was repeated to calculate the ensembled 2-D fall zone distribution for the eastern red bat fatality with e = 0.1. The two ensemble distributions (e = 0 and 0.1) were combined to give the final 2-D ensembled fall zone distribution of the eastern red bat when bat strikes are uniformly distributed on the rotor plane (Figure 11). The red dot plotted on the final ensemble fall zone distribution displays the carcass location reported in the survey data. To identify the bats impacting the ground near the surveyed location, a window of 10 × 10 m was drawn around the

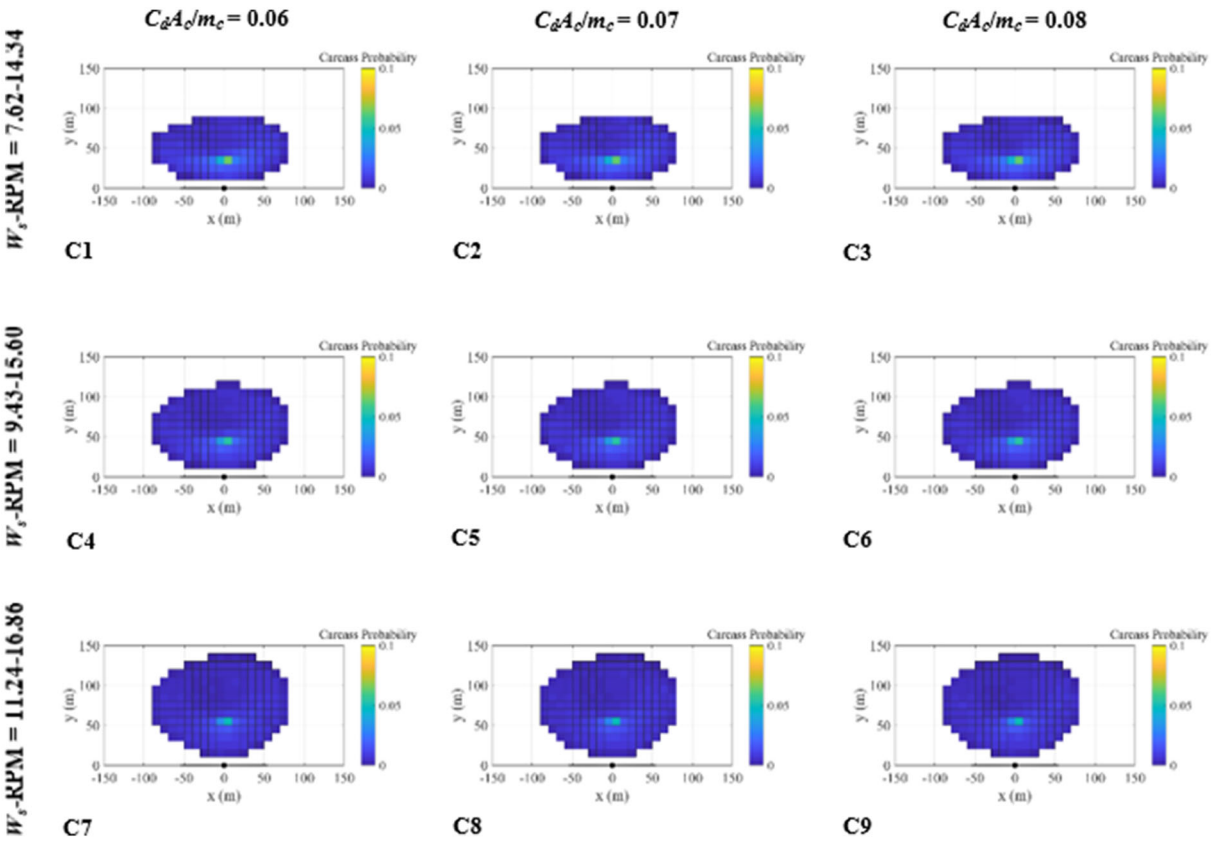

FIGURE 10 Fall zone distributions from nine combinations for the eastern red bat (e = 0) (C1 → C3, C4 → C6 and C7 → C9: (C_dA_c/m_c) varies, C1 → C7, C2 → C8 and C3 → C9: W_s vs. RPM varies)

FIGURE 11 Ensembled fall zone distribution

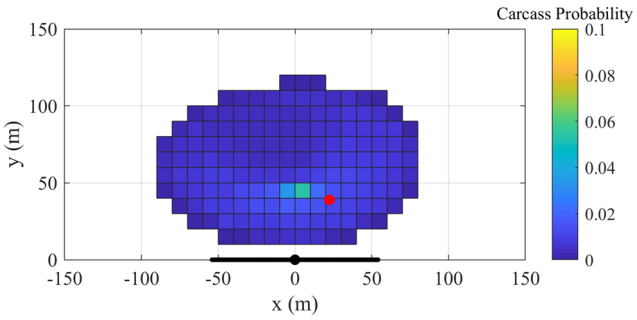

carcass. The radial and angular position of the bats in the marked window was computed and backtracked to the rotor plane to determine the plausible region of the strike location that most likely led to fatality location reported in the survey.

After finding the plausible radial and angular positions of bat strikes on the rotor, the 3-D fall trajectories were computed for bats at higher resolution (0.1 m and 0.1°) on the rotor, resulting in 7,212 carcasses landing close to the bat survey location. The radial and angular position of bats falling within a window of 5 × 5 m centred at the surveyed location was identified. Using these results, a cumulative probability distribution contour[32] of bat strike locations was calculated (Figure 12). The radial and angular position of highest bat strike probability on the rotor was identified as r = 13 m and θ = 18°. The ballistics model was run to compute the back-trajectory from the carcass ground location to the rotor. Figure 13 shows the 3-D back-trajectory of the eastern red bat carcass from the most probable strike location on the rotor. Finally, the computed impact location on the ground was found to be in agreement with the reported survey.

The proposed bat strike location estimation methodology was applied for the six remaining selected bat fatalities described in Table 1. The cumulative probability distribution contour of bat likely strike location was computed for each surveyed carcass to evaluate the most likely strike locations on the rotor. The bat strike contours and corresponding 3-D back-trajectories of the remaining bat fatalities are provided in the

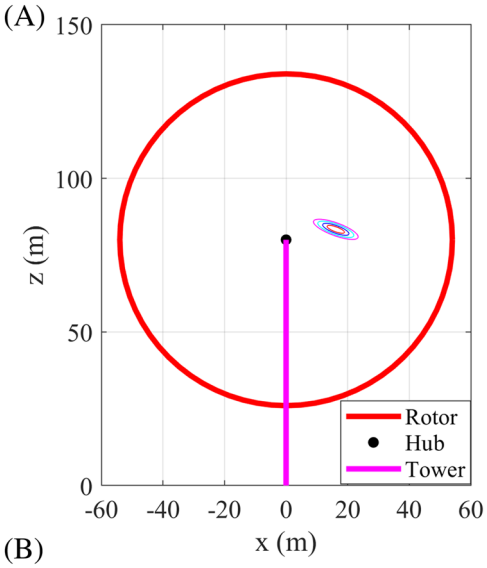

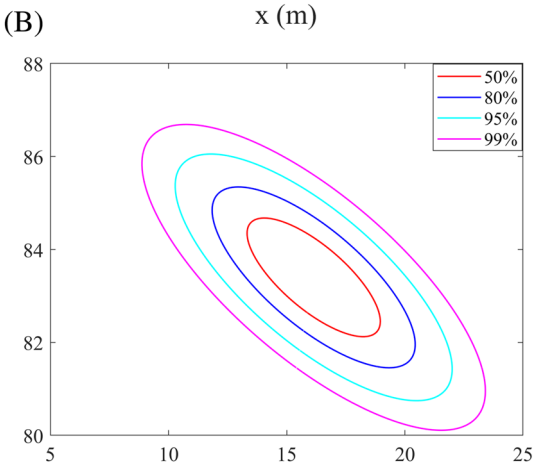

FIGURE 12 (A) Cumulative probability distribution contour of bat likely strike locations on the rotor plane and (B) zoomed in region of the likely bat strike locations

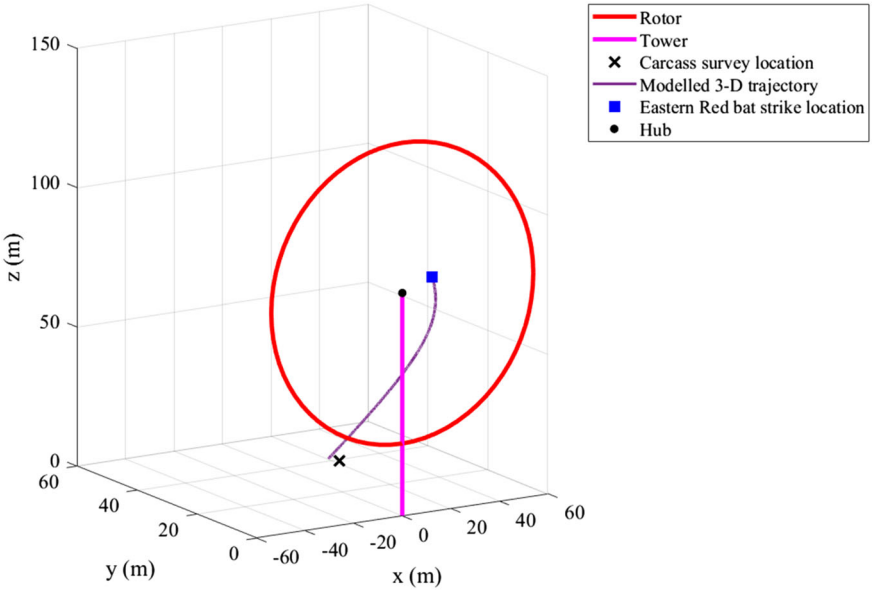

FIGURE 13 Three-dimensional (3-D) back-trajectory for the eastern red bat fatality

supporting information. Figure 14 shows the resulting fall trajectories for all the bat fatalities listed in Table 1. The star symbol in the figure represents the hoary bat strike locations, whereas square symbol represents the eastern red bat strike locations. Simulated impacts on the ground based on the most probable strike locations were found to be within 2 m of each of the surveyed carcasses.

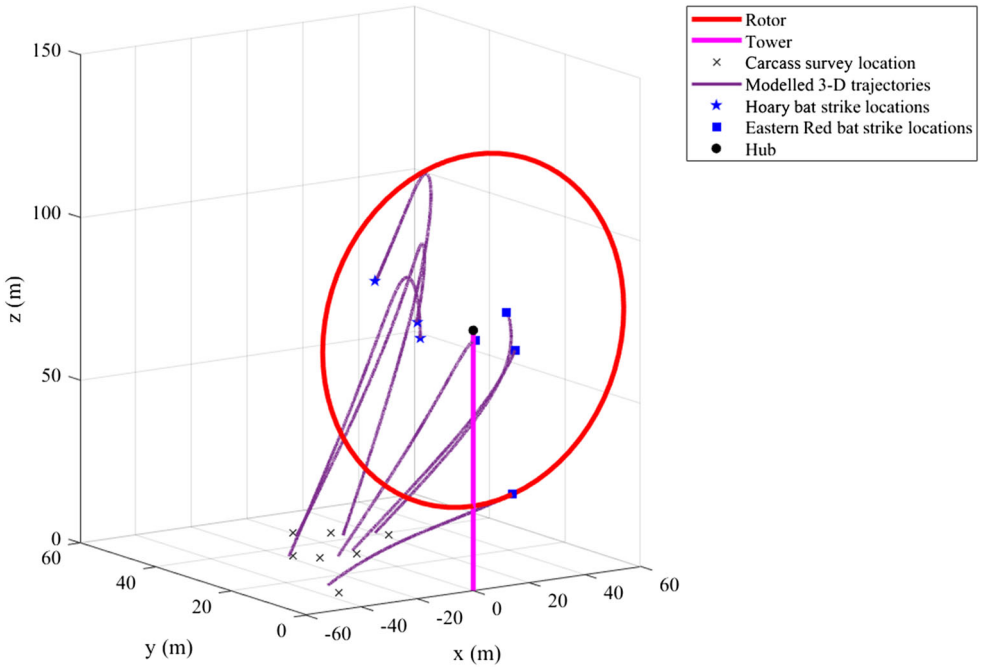

FIGURE 14 Modelled 3-D trajectories of seven selected bat fatalities

7 | CONCLUSIONS AND POTENTIAL OF PROPOSED MODEL

Wind turbine operators require robust methods to guide the carcass survey efforts to determine the appropriate extent of the surveys and the most likely locations where bat carcasses are likely to be found around turbines. The 2018 carcass survey and SCADA data from an Iowa wind farm were analysed, and it was discovered that carcasses fall downward of wind turbine. The effect of wind drift was identified as a significant factor determining how bat carcasses fall after blade strike, which needs to be accounted to accurately estimate the carcass ground impact locations. A new ballistics model is proposed to simulate carcass 3-D fall trajectories for given bat biophysical and aerodynamic characteristics, wind speed and corresponding turbine operation, and bat flight characteristics. Tests were conducted to determine the sensitivity of carcass fall trajectories with respect to the input parameters of the ballistics model. The sensitivity tests showed that larger values of the bat carcass parameter resulted in greater downwind drift whereas smaller values of the carcass parameter resulted in larger in-plane displacement. The wind speed and corresponding RPM influences the downwind distance more than the in-plane distance, indicating a greater influence of wind drift compared to inertia. Bat flight speed and bat strike angle were found to primarily affect the trajectory of carcasses with smaller carcass parameter. The coefficient of restitution was found to have limited effect on the impact patterns on the ground. The turbine model was found to affect the impact pattern on the ground, covering a larger area proportional to the turbine blade length and total turbine height. These are interesting findings, but it is worth mentioning here that the sensitivity analysis results are based on a limited sample of bat carcasses, to ensure strict control of the input data. We recommend additional research to determine how representative these results are for wind farms with different bat species having different behaviour, biophysical and aerodynamic characteristics.

The proposed ballistics model was used to identify the likely bat strike locations on the rotor for surveyed carcasses. Due to uncertainty in the precise wind speed and corresponding turbine operational conditions at the time of blade strike, time series from SCADA records were analysed to identify a range of input parameters. The bat carcass' biophysical and aerodynamic characteristics were also not known, and therefore, a parameter matrix was used to compute the ensembled fall zone distribution of bats, using the 3-D ballistics model to incorporate the uncertainty into the model. The simulated carcasses falling in a window around the survey location were backtracked to determine the bat strike location cumulative frequency distribution to provide an estimate of the most probable strike location on the rotor plane. The analysis revealed that the bats collide with the turbine blades at approximately hub height, over the full range of the rotor radius. However, it is important to highlight the findings are based on limit data and more study is needed to determine if the results are representative for other bat species and wind farm projects.

The proposed model has the potential to be useful for several applications to understand the direct impact of wind facilities on bats as well as birds. Future research could consider combining this model with an uncertainty propagation technique such as Monte-Carlo to introduce a methodology to guide survey visits at individual turbines incorporating the nightly yaw variation or in the whole wind farm during the during the

autumn season. The model has the potential to improve the fatality estimates through a weighing function accounting for unsearched areas and multiplying it with modelled fatality estimates to yield improved fatality estimates. The model may also be applied to wind farms located in different geographic locations encountering different meteorological conditions and bat species.

Maximum turbine height is a useful predictor of maximum distance travelled by carcasses. The larger the turbine height, the more time carcass takes to reach to ground, increasing the time for wind drift to carry the carcass, resulting in larger fall distances, particularly for lighter carcasses with large carcass parameter. Therefore, variation of turbine height is an important factor generally informing the distance carcasses may fall. A useful consideration as taller turbines is installed in the future. However, the proposed model can account for details of meteorology, and turbine operating characteristics that we show can significantly affect the fall zone range. The sensitivity analysis results suggest that bats fall further from the turbine at higher wind speeds. This is an important finding and has important implications in recommending large search plots during curtailment studies to identify the bat fatalities. Turbine curtailment causes the turbines to shut down at low speeds and operate only at higher wind speeds. This results in occurrence of bat fatalities at high wind speed only and in the absence of large search plots, these are very likely to be missed. This model is useful to account for this curtailment bias.

The model may be further validated using video surveillance of bat strikes and measurements of fall trajectories and pre-strike flight velocities. The strike distribution may be further refined based on measurements of bat activity near the rotor to determine their behaviour around the turbine blades and video recorded strike locations. This could aid development of a quantitative model framework for predicting collision risk and be used to evaluate deterrent technologies. The 3-D ballistics model can also be applied to other avian such as birds. However, lift force, which is not significant for bats, would need to be accounted for with larger bird carcasses.

ACKNOWLEDGMENTS

The study was conducted with financial support from MidAmerican Energy Company (MEC), and with input from scientists at the U.S. Fish & Wildlife Service (USFWS) in support of development of a Habitat Conservation Plan for Wind Energy Facilities in Iowa.

CONFLICT OF INTEREST

The authors declare no conflict of interest. The funders had no role in the study design, analysis of the data, decision to publish or preparation of the manuscript.

AUTHOR CONTRIBUTIONS

SP conducted the study as part of his doctoral research supervised by CDM. CDM conceptualized the research and acquired financial support. SP conducted data analysis and produced final results, figures and original draft of the manuscript. SP and CDM interpreted the analysis results and reviewed and revised the final version of the manuscript.

DATA AVAILABILITY STATEMENT

Data and MATLAB code are available upon request from the corresponding author.

ORCID

Shivendra Prakash https://orcid.org/0000-0002-2720-4957
Corey D. Markfort https://orcid.org/0000-0003-3168-9149

REFERENCES

1. Chu S, Majumdar A. Opportunities and challenges for a sustainable energy future. *Nature*. 2012;488(7411):294-303. https://doi.org/10.1038/nature11475
2. Intergovernmental Panel on Climate Change [IPCC]. Summary for policy makers. In: *Climate Change 2014: Mitigation of Climate Change Contribution of Working Group III to the Fifth Assessment Report of the Intergovernmental Panel on Climate Change*. Cambridge, UK: Cambridge University Press; 2014 https://www.ipcc.ch/site/assets/uploads/2018/02/ipcc_wg3_ar5_full.pdf
3. Kuvlesky WP, Brennan LA, Morrison ML, Boydston KK, Ballard BM, Bryant FC. Wind energy development and wildlife conservation: challenges and opportunities. *J Wildl Manage*. 2007;71(8):2487-2498. https://doi.org/10.2193/2007-248
4. Banerjee A, Prehoda E, Sidortsov R, Schelly C. Renewable, ethical? Assessing the energy justice potential of renewable electricity. *AIMS Energy*. 2017;5(5):768-797. https://doi.org/10.3934/energy.2017.5.768
5. Gibson L, Wilman EN, Laurance WF. How green is 'green' energy? *Trends Ecol Evol*. 2017;32(12):922-935. https://doi.org/10.1016/j.tree.2017.09.007
6. Zerrahn A. Wind power and externalities. *Ecol Econ*. 2017;141:245-260. https://doi.org/10.1016/j.ecolecon.2017.02.016
7. Arnett EB, Baerwald EF. Impacts of wind energy development on bats: implications for conservation. In: Adams RA, Pedersen SC, eds. *Bat evolution, ecology, and conservation*. Springer; 2013:435-456.
8. Zimmerling JR, Francis CM. Bat mortality due to wind turbines in Canada. *J Wildl Manag*. 2016;80(8):1360-1369. https://doi.org/10.1002/jwmg.21128
9. Cryan PM. Wind turbines as landscape impediments to the migratory connectivity of bats. *Environ Law*. 2011;41:355-370.

10. Hayes MA. Bats killed in large number of United States wind energy facilities. *Bioscience*. 2013;63(12):975-979. https://doi.org/10.1525/bio.2013.63.12.10
11. Smallwood KS. Comparing bird and bat fatality-rate estimates among North-American wind-energy projects. *Wildl Soc Bull*. 2013;37(1):19-33. https://doi.org/10.1002/wsb.260
12. Frick WF, Baerwald EF, Pollock JF, et al. Fatalities at wind turbines may threaten population viability of a migratory bat. *Biol Conserv*. 2017;209:172-177. https://doi.org/10.1016/j.biocon.2017.02.023
13. American Wind Energy Association (AWEA). https://www.awea.org/wind-101/basics-of-windenergy/wind-facts-at-a-glance. Accessed December 8, 2019 2019.
14. Smallwood KS, Bell DA. Effect of wind turbine curtailment on bird and bat fatalities. *J Wild Manage*. 2020;84(4):685-696. https://doi.org/10.1002/jwmg.21844
15. Kunz TH, Arnett EB, Erickson WP, et al. Ecological impacts of wind energy development on bats: questions, research needs, and hypotheses. *Front Ecol Environ*. 2007;5(6):315-324. https://doi.org/10.1890/1540-9295(2007)5[315:EIOWED]2.0.CO;2
16. Bernard E, Paese A, Machado RB, Aguiar LMS. Blown in the wind: bats and wind farms in Brazil. *Nat Conserv*. 2014;12(2):106-111. https://doi.org/10.1016/j.ncon.2014.08.005
17. Voigt CC, Lindecke O, Schönborn S, Kramer-Schadt S, Lehmann D. Habitat use of migratory bats killed during autumn at wind turbines. *Ecol Appl*. 2016;26(3):771-783. https://doi.org/10.1890/15-0671
18. Aronson J, Richardson E, MacEwan K, et al. South African good practice guidelines for operational monitoring for bats at wind energy facilities. South African Bat Assessment Advisory Panel, Johannesburg, South Africa. 2014. https://tethys.pnnl.gov/publications/south-african-good-practice-guidelines-operational-monitoring-bats-wind-energy
19. Hull CL, Cawthen L. Bat fatalities at two wind farms in Tasmania, Australia: bat characteristics and spatial and temporal patterns. *N Z J Zool*. 2013;40(1):5-15. https://doi.org/10.1080/03014223.2012.731006
20. Hull CL, Muir S. Search areas for monitoring bird and bat carcasses at wind farms using a Monte-Carlo model. *Australas J Environ Manag*. 2013;17(2):77-87. https://doi.org/10.1080/14486563.2010.9725253
21. Biswas S, Taylor P, Salmon JA. Model for ice throw trajectories from wind turbines. *Wind Energy*. 2011;15(7):889-901. https://doi.org/10.1002/we.519
22. Sarlak H, Sørensen JN. Characterization of blade throw from a 2.3 MW horizontal axis wind turbine upon failure. AIAA Sci Tech, 53rd AIAA Aerospace Sciences Meeting, 5–9 January 2015, Kissimmee, Florida. 2015; https://doi.org/10.2514/6.2015-1494
23. Cryan PM, Gorresen PM, Hein DH, et al. Behavior of bats at wind turbines. *PNAS*. 2014;111(42):15126-15131. https://doi.org/10.1073/pnas.1406672111
24. Arnett EB, Schirmacher M, Huso MMP, Hayes JP. Effectiveness of changing wind turbine cut-in speed to reduce bat mortalities at wind facilities. An annual report submitted to the Bats and Wind Energy Cooperative. Bat Conservation International. Austin, Texas, USA, 2010. https://tethys.pnnl.gov/sites/default/files/publications/Arnett_and_Schirmacher_2010.pdf
25. Martin JE, Politano MS, Prakash S, Carrica PM, Markfort CD. Optimizing bat carcass search areas using a CFD-Lagrangian modelling approach. In Appendix E – Particle Distribution Model, MidAmerican Energy Company Habitat Conservation Plan for Wind Energy Facilities I-X in Iowa https://www.fws.gov/midwest/RockIsland/te/MidAmericanHCP.html
26. Prakash S, Markfort CD. Experimental investigation of aerodynamic characteristics of bat carcasses after collision with a wind turbine. *Wind Energ Sci*. 2020;5(2):745-758. https://doi.org/10.5194/wes-5-745-2020
27. Hayward B, Davis R. Flight speed in western bats. *J Mammal*. 1964;45(2):236-242.
28. McCracken GF, Safi K, Kunz TH, Dechmann DK, Swartz SM, Wikelski M. Airplane tracking documents the fastest flight speeds recorded for bats. *R Soc Open Sci*. 2016;3(11):160398. https://doi.org/10.1098/rsos.160398
29. Summary of Mist-Net Captures. Appendix D. MidAmerican HCP addendum technical reports. https://www.fws.gov/midwest/endangered/permits/hcp/pdf/MidAmericanHCP_Addendum_Technical%20Reports.pdf. Accessed March 7, 2019.
30. Genter DL, Jurist KA. Bats of Montana. http://mtnhp.org/animal/reports/mammals/batsummary.pdf. Accessed December 22, 2019.
31. Author. Special guide to Vermont bats. https://vtfishandwildlife.com/sites/fishandwildlife/files/documents/Learn%20More/Living%20with%20Wildlife/Bats/VT_Bat_Species_ID.pdf. Accessed December 22, 2019 2019.
32. Gold D. Plotting probability ellipses for bivariate Normal distributions. https://waterprogramming.wordpress.com/2016/11/07/plotting-probability-ellipses-for-bivariate-normal-distributions/

SUPPORTING INFORMATION

Additional supporting information may be found online in the Supporting Information section at the end of this article.

How to cite this article: Prakash S, Markfort CD. Development and testing of a three-dimensional ballistics model for bat strikes on wind turbines. *Wind Energy*. 2021;1–19. https://doi.org/10.1002/we.2638